

Dedicated to the memory of Academician Il'ya Iosifovich Moiseev

Cyclometallation of the Dimethylamide Ligand in the Reaction of $\text{Ta}(\text{NMe}_2)_5$ with CS_2

P. A. Petrov^a, *, A. V. Rogachev^a, I. V. El'tsov^b, T. S. Sukhikh^a, Yu. A. Laricheva^a,
P. A. Abramov^a, and M. N. Sokolov^a

^a Nikolaev Institute of Inorganic Chemistry, Siberian Branch, Russian Academy of Sciences, Novosibirsk, Russia

^b Novosibirsk State University, Novosibirsk, Russia

*e-mail: panah@niic.nsc.ru

Received April 2, 2021; revised May 5, 2021; accepted May 6, 2021

Abstract—The reaction of $\text{Ta}(\text{NMe}_2)_5$ with CS_2 resulted in the isolation of azametallacyclopropane complex $[\text{Ta}(\text{MeDtc})_3(\eta^2\text{-CH}_2\text{NMe})]$ (**I**, MeDtc = dimethyldithiocarbamate), which was characterized by X-ray diffraction in the solvent-free form and as a toluene solvate (CCDC nos. 2005837 (**I**), 2049693 (**I**· $0.5\text{C}_7\text{H}_8$)) and by NMR spectroscopy and DFT calculations.

Keywords: tantalum, amides, dithiocarbamates, X-ray diffraction

DOI: 10.1134/S1070328421100055

INTRODUCTION

Metal amides are important for modern coordination chemistry and are precursors of many other ligands [1]. In addition, dialkylamides (most often, dimethylamides) of early transition metals and their mixed-ligand derivatives are precursors of thin films of metal nitrides obtained by chemical vapor deposition (CVD) [2]. The presence of carbon impurity (both free and metal-bound) in the obtained films was attributed to its formation during precipitation of azametallacyclopropanes upon elimination of the methyl group proton. In addition, azametallacyclopropane complexes are assumed to be intermediates of a number of catalytic reactions, e.g., hydroamination of alkenes [3, 4]. Structural data were reported for several complexes of early transition metals with the $\text{CH}_2\text{NMe}^{2-}$ anion coordinated in both terminal and bridging fashions [4–8]. This work is devoted to the synthesis and studies of tantalum azametallacyclopropane complex $[\text{Ta}(\text{MeDtc})_3(\eta^2\text{-CH}_2\text{NMe})]$.

EXPERIMENTAL

The synthesis was carried out in an inert atmosphere using standard Schlenk glassware. The solvents were dehydrated and degassed by refluxing and distillation under argon using appropriate drying agents [9]. CS_2 (Acros) was dried over 3A molecular sieves and then degassed. The NMR spectra were measured on a Bruker Avance III 500 spectrometer operating at 500.03 MHz for ^1H and at 125.73 MHz for ^{13}C ; solvent

signals were used as the standards ($\delta_{\text{H}} = 3.58$ ppm, $\delta_{\text{C}} = 67.21$ ppm) [10]. IR spectra were measured for KBr pellets on a SCIMITAR FTS 2000 instrument. Elemental analysis was carried out at the Analytical Laboratory of the Nikolaev Institute of Inorganic Chemistry, Siberian Branch, Russian Academy of Sciences.

Synthesis of $[\text{Ta}(\text{MeDtc})_3(\eta^2\text{-CH}_2\text{NMe})]$ (I). $\text{Ta}(\text{NMe}_2)_5$ (Dalkhim, Russia) (443 mg, 1.10 mmol) was placed into a Schlenk vessel, and toluene (20 mL) and CS_2 (200 μL , 253 mg, 3.32 mmol) were successively condensed into the vessel at a reduced pressure with cooling. After spontaneous warming up of the mixture from -196°C to room temperature, a light-colored solid precipitated, and the color of the precipitate gradually changed to brown. The suspension was heated at 65°C for 24 h, cooled, and evaporated to dryness. The residue was extracted with toluene (15 mL), and the yellow extract was filtered through a glass filter (G4) and sealed in an L-shaped tube. After slow evaporation of the solvent, yellow crystals of **I**· $0.5\text{C}_7\text{H}_8$, suitable for X-ray diffraction, were formed in the free leg of the tube. The yield was 90 mg (15%).

For $\text{C}_{11}\text{H}_{23}\text{N}_4\text{S}_6\text{Ta}$

Anal. calcd., %	C, 22.60	H, 3.97	N, 9.58
Found, %	C, 22.15	H, 3.85	N, 9.50 ¹

¹ Analysis was performed for a sample of **I**· $0.5\text{C}_7\text{H}_8$ dried in a dynamic vacuum to a constant weight.

¹H NMR (500 MHz; THF; δ , ppm): 2.22 (s, 2H, CH_2), 3.27 (m, 18H, CH_3^{Dtc}), 3.96 (s, 3H, CH_3). ¹³C NMR (126 MHz; THF; δ , ppm): 39.0 (CH_3^{Dtc}), 48.2 (CH_3NCH_2), 56.0 (CH_3NCH_2), 204.7 (Me_2NCS_2), 206.7 (Me_2NCS_2).

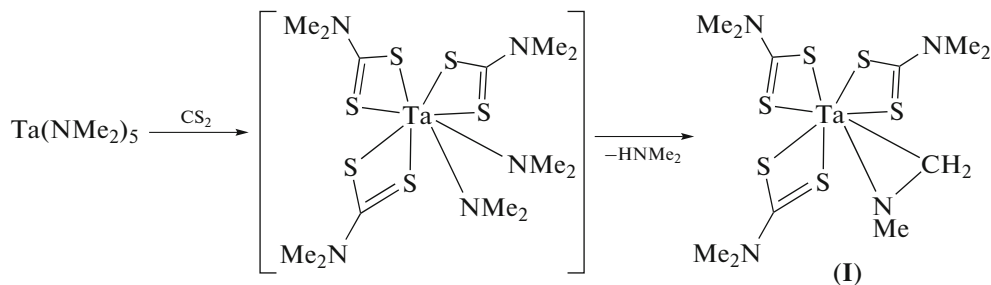
IR (KBr; ν , cm^{-1}): 2926 w, 2855 w, 1533 vs, 1447 m, 1395 vs, 1247 s, 1147 s, 1049 m, 996 m, 982 m, 899 w, 574 w.

X-ray diffraction. The single crystals of the solvent-free form of **I** were formed as an impurity in the previously reported synthesis of $[\text{Ta}(\text{MeDtc})_4](\text{MeDtc})\cdot\text{C}_7\text{H}_8$ [11]. The measurements for **I** and **I**·0.5C₇H₈ were carried out by the standard procedure on a Bruker-Nonius X8 APEX automated four-circle diffractometer (CCD array detector, $\lambda = 0.71073 \text{ \AA}$, graphite monochromator). The reflection intensities were measured by φ -scanning of narrow (0.5°) frames. The absorption corrections were applied empirically (SADABS) [12]. The structures were solved by the SHELXT program [13] and refined by the SHELXL program [14] in the anisotropic approximation for non-hydrogen atoms using the Olex2 software shell [15]. The hydrogen atoms were located geometrically and refined in the rigid body approximation. The crystallographic characteristics of the complex and X-ray experiment details are summarized in Table 1. The crystallographic data are deposited with the Cambridge Crystallographic Data Centre (CCDC no. 2005837 (**I**) and no. 2049693 (**I**·0.5C₇H₈) and are available from <http://www.ccdc.cam.ac.uk/conts/retrieving.html>.

Quantum chemical calculations were performed by the DFT method using the ADF2019 software package [16, 17], the TZ2P full-electron basis set, and VWN (local density approximation) [18] and BP86 (generalized gradient approximation) [19–21] functionals. The relativistic effects were considered by the ZORA method [22].

RESULTS AND DISCUSSION

The insertion of CS₂ into the M–N bond of early transition metal amides is a general method for the synthesis of metal dithiocarbamates [23, 24]. Previously, we obtained two solvates $[\text{Ta}(\text{MeDtc})_4](\text{MeDtc})$ with a dodecahedral environment of the central atom by the reaction of Ta(NMe₂)₅ with excess CS₂ [11]. Apart from $[\text{Ta}(\text{MeDtc})_4](\text{MeDtc})$ formed as the major product, the reaction of Ta(NMe₂)₅ with CS₂ gave $[\text{Ta}(\text{MeDtc})_3(\eta^2\text{-CH}_2\text{NMe}_2)]$ (**I**) as a minor product formed in a low yield. Obviously, this product is formed because of the steric overcrowding of the coordination unit in the intermediate $[\text{Ta}(\text{MeDtc})_3(\text{NMe}_2)_2]$, which then eliminates Me₂NH (Scheme 1).



Scheme 1.

Complex **I** crystallizes in the hexagonal space group *P*6₁. The geometry of the coordination polyhedron is close to dodecahedral, which was detected earlier in the $[\text{Ta}(\text{MeDtc})_4]^+$ cations [11]. The structure of **I** is shown in Fig. 1. The angles between the chelate ring planes of neighboring ligands (MeDtc^- and $\text{CH}_2\text{NMe}^{2-}$) are close to 90° (88.1°–92.7°). Each dithiocarbamate ligand has two somewhat different Ta–S bonds (2.59 and 2.64 Å), which is usual for this class of ligands (Table 2). The $\angle\text{STA}\text{S}$ chelate angles (66.93(10)°–67.36(9)°) are also similar to those known from the literature. The Ta(1)–N(4) distances (1.955(10) Å) are somewhat shorter than this distance in Ta(NMe₂)₅ (average, 2.017 Å); the Ta(1)–C(10) distance is 2.206(11) Å. A distinctive feature of **I** is small $\angle\text{N}(4)\text{Ta}(1)\text{C}(10)$ chelate angle (39.1(4)°),

which is close to the values known for other complexes with the terminal $\text{CH}_2\text{NMe}^{2-}$ ligand (39.4°–40.0°). For comparison, N-protonated molybdenum(IV) azametallacyclopropane complex $[\text{Mo}(\text{Me}_2\text{Pz})_3(\text{HMe}_2\text{Pz})(\eta^2\text{-CH}_2\text{NHMe})]$ (**II**; HMe₂Pz = 3,5-dimethylpyrazole) has equally small chelate angle of the CH_2NHMe^- ligand (39.0(2)°) [25]. Meanwhile, the Mo–N distance (2.145(3) Å) in **II** is markedly longer than the Ta–N distance in **I** (1.955(10) Å), although the Mo⁴⁺ and Ta⁵⁺ ionic radii are virtually equal. One more difference is the sum of angles at the azametallacyclopropane N atom, which is 358.0° in **I**, unambiguously indicating the absence of a proton at this atom, and 318.5° in **II** (without considering the H atom).

Table 1. Crystallographic data and structure refinement details for **I** and **I**·0.5C₇H₈

Parameter	Value	
	I	I ·0.5C ₇ H ₈
Molecular formula	C ₁₁ H ₂₃ N ₄ S ₆ Ta	C ₂₉ H ₅₄ N ₈ S ₁₂ Ta ₂
<i>M</i>	584.64	1261.42
System, space group	Hexagonal, <i>P</i> 6 ₁	Monoclinic, <i>P</i> 2 ₁ /c
Temperature, K	296(2)	150(2)
<i>a</i> , Å	9.813(3)	13.8012(15)
<i>b</i> , Å	9.813(3)	11.7849(12)
<i>c</i> , Å	39.048(13)	29.638(3)
α, deg	90	90
β, deg	90	102.878(4)
γ, deg	120	90
<i>V</i> , Å ³	3256(2)	4699.3(9)
<i>Z</i>	6	4
μ, mm ⁻¹	5.641	5.218
Crystal size, mm	0.21 × 0.12 × 0.12	0.3 × 0.25 × 0.2
<i>F</i> (000)	1716.0	2488.0
Data collection range for 2θ, deg	4.794–51.626	2.82–52.744
Range of indices <i>h</i> , <i>k</i> , <i>l</i>	–11 ≤ <i>h</i> ≤ 7, –3 ≤ <i>k</i> ≤ 12, –47 ≤ <i>l</i> ≤ 37	–17 ≤ <i>h</i> ≤ 17, –14 ≤ <i>k</i> ≤ 14, –37 ≤ <i>l</i> ≤ 37
Number of measured, unique, and observed (<i>I</i> > 2σ(<i>I</i>)) reflections	7792, 3549, 3136	48169, 9611, 8347
GOOF	0.986	1.044
<i>R</i> _{int}	0.0448	0.0304
<i>R</i> ₁ , <i>wR</i> ₂ (<i>I</i> > 2σ(<i>I</i>))	<i>R</i> ₁ = 0.0367, <i>wR</i> ₂ = 0.0609	<i>R</i> ₁ = 0.0387, <i>wR</i> ₂ = 0.0967
<i>R</i> ₁ , <i>wR</i> ₂ (all reflections)	<i>R</i> ₁ = 0.0444, <i>wR</i> ₂ = 0.0635	<i>R</i> ₁ = 0.0456, <i>wR</i> ₂ = 0.1021
Flack parameter	0.012(12)	
Number of refined parameters	199	463
Number of constrains	1	0
Δρ _{max} /Δρ _{min} , e Å ⁻³	0.64/–0.51	2.71/–1.42

Complex **I** was obtained in a slightly higher yield (15%) by the reaction of Ta(NMe₂)₅ with CS₂ taken in 1 : 3 ratio in toluene. Despite the reactant ratio, this reaction (like the reaction with excess CS₂, see [11]) gives predominantly poorly soluble [Ta(^{Me}Dtc)₄][–](^{Me}Dtc)·0.5C₇H₈. The removal of this product from the toluene solution by filtration gave the crystals of solvate **I**·0.5C₇H₈, which contains two crystallographically independent molecules of **I**. The geometric characteristics of the complex in the solvate and solvent-free forms are similar (Table 2). NMR data are in full agreement with crystallographic data.

The electronic structure of complex **I** was studied by quantum chemical calculations. Comparison of the averaged values of the optimized structural parameters

with X-ray diffraction data is presented in Table 3. The calculated interatomic distances are in good agreement with the X-ray diffraction data.

Geometry optimization leads to a slight increase in the symmetry of the optimized structure compared to the original one. Each ligand in the optimized structure is planar (without considering the H atom). The CH₂NMe²[–] moiety is located in one plane with the opposing dithiocarbamate. This brings about a situation in which the HOMO and HOMO-1 orbitals can be considered as virtually degenerate, due to symmetry increase (Fig. 2). These orbitals are close in energy (the difference is less than 0.05 eV), have similar shapes, but differ in the composition (Table 4). However, both orbitals are composed of both the metal and

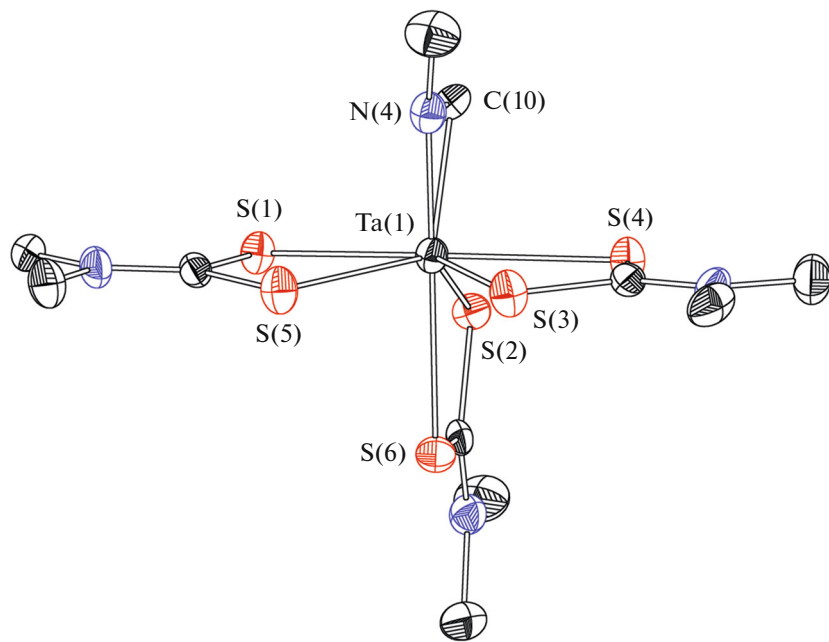


Fig. 1. Structure of complex **I** (thermal ellipsoids at 30% probability level; hydrogen atoms are omitted).

Table 2. Selected bond lengths (Å) and bond angles (deg) in structures of **I** and **I**·0.5C₇H₈

I		I ·0.5C ₇ H ₈			
		molecule 1		molecule 2	
Bond	<i>d</i> , Å	Bond	<i>d</i> , Å	Bond	<i>d</i> , Å
Ta(1)–N(4)	1.955(10)	Ta(1)–N(7)	1.925(5)	Ta(2)–N(8)	1.968(6)
Ta(1)–C(10)	2.206(11)	Ta(1)–C(71)	2.169(6)	Ta(2)–C(81)	2.172(8)
Ta(1)–S(4)	2.587(3)	Ta(1)–S(11)	2.5627(14)	Ta(2)–S(41)	2.6185(15)
Ta(1)–S(10)	2.586(3)	Ta(1)–S(12)	2.6001(15)	Ta(2)–S(42)	2.5913(16)
Ta(1)–S(2)	2.594(3)	Ta(1)–S(21)	2.5667(15)	Ta(2)–S(51)	2.6134(16)
Ta(1)–S(5)	2.636(3)	Ta(1)–S(22)	2.6403(15)	Ta(2)–S(52)	2.5437(15)
Ta(1)–S(3)	2.639(3)	Ta(1)–S(31)	2.5885(16)	Ta(2)–S(61)	2.5968(16)
Ta(1)–S(6)	2.644(3)	Ta(1)–S(32)	2.6044(15)	Ta(2)–S(62)	2.5706(17)
N(4)–C(10)	1.412(15)	N(7)–C(71)	1.318(10)	N(8)–C(81)	1.330(11)
N(4)–C(11)	1.430(15)	N(7)–C(72)	1.466(8)	N(8)–C(82)	1.441(11)
Angle	ω, deg	Angle	ω, deg	Angle	ω, deg
S(1)Ta(1)S(5)	66.93(10)	S(11)Ta(1)S(12)	67.05(5)	S(42)Ta(2)S(41)	66.44(5)
S(4)Ta(1)S(3)	67.09(11)	S(21)Ta(1)S(22)	68.34(5)	S(52)Ta(2)S(51)	68.03(5)
S(2)Ta(1)S(60)	67.36(9)	S(31)Ta(1)S(32)	66.44(6)	S(62)Ta(2)S(61)	66.43(5)
N(4)Ta(1)C(10)	39.1(4)	N(7)Ta(1)C(71)	36.9(3)	N(8)Ta(2)C(81)	37.1(3)
N(4)C(10)Ta(1)	60.8(6)	N(7)C(71)Ta(1)	61.4(3)	N(8)C(81)Ta(2)	63.1(4)
Ta(1)N(4)C(10)	80.1(6)	C(71)N(7)Ta(1)	81.7(4)	C(81)N(8)Ta(2)	79.8(4)

(to one or another extent) all ligands. This mixed character of HOMO and HOMO-1 differs fundamentally from the shape and composition of HOMO-2, which is almost completely centered on the sulfur atoms of dithiocarbamate ligands with a minor contribution of the nitrogen atom of the CH_2NMe^2- moiety. The lowest unoccupied orbitals LUMO and LUMO+1 are not degenerate, both being ligand-centered; however, unlike LUMO+1, LUMO has contributions of all ligands including the azametallacyclopropane moiety. The HOMO and HOMO-1 compositions mainly correspond to binding of Ta *d*-orbitals to the appropriate orbitals of the CH_2NMe^2- ligand. The orbitals responsible for binding to sulfur atoms are located lower in energy and are not shown in Fig. 2.

Topological electron density analysis by the ELF and QTAIM methods [26, 27] was carried out to identify the character of binding of Ta to both types of ligands and binding inside the azametallacyclopropane moiety (Table 5). From the ELF data and critical point analysis, it follows that metal–ligand bonds have the donor–acceptor nature (coordination bonds) for all ligands. The electron density at the bond critical points is moderate: $\nabla^2\rho_{av} > 0$, $V(r) < 0$, $H(r) < 0$. The

Table 3. Average bond lengths (Å) in **I** according to X-ray diffraction data (solvent-free form) and DFT calculations

Bond	X-ray diffraction	DFT
Ta–S	2.614	2.612
C–S	1.729	1.722
N–CS ₂ (Dtc)	1.330	1.350
N–CH ₃ (Dtc)	1.466	1.458
C–N*	1.412	1.416
Ta–N*	1.955	1.939
Ta–C*	2.206	2.207

* Bond lengths in the azametallacyclopropane moiety.

critical points of all bonds that include Ta are shifted along the line of binding towards the metal.

Thus, the tantalum azametallacyclopropane complex $[\text{Ta}^{(\text{Me})\text{Dtc}}_3(\eta^2\text{-CH}_2\text{NMe})]$ was isolated and characterized by X-ray diffraction and NMR and IR spectroscopy. The electronic structure of the complex

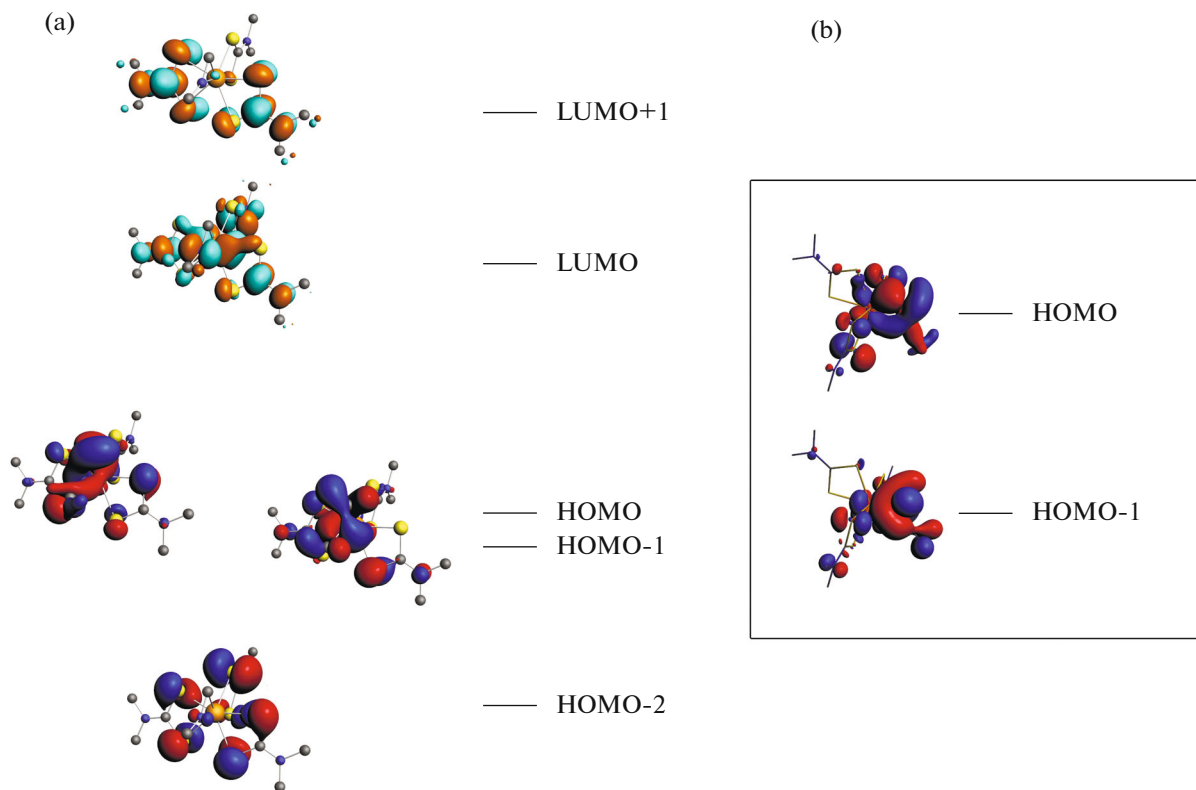


Fig. 2. (a) Diagram of energy levels and frontier orbitals of complex **I**; (b) projection of HOMO and HOMO-1 (for more clear demonstration of sigma bonds, hydrogen atoms are omitted).

Table 4. Energy (eV) and AO contributions to the MO of complex I

Orbital	Energy	Composition, %				
		Ta	C	N	S	H
LUMO+1	−1.62		57.03	18.70	19.27	1.02
LUMO	−1.74	25.78	34.11	21.78	5.47	0.90
HOMO	−4.67	14.69	26.98	9.58	26.67	4.03
HOMO-1	−4.72	11.89	9.07	38.14	13.44	15.91
HOMO-2	−4.92			2.98	89.25	

Table 5. Topological descriptors of the QTAIM theory*

Bond	Length, Å	BP, Å	ρ_{av}	$\nabla^2\rho_{av}$	G_{av}	V_{av}	H_{av}	H_{av}/ρ_{av}	$ V_{av} /G_{av}$	$ V_{av} $
Ta—N**	1.939	1.949	0.151	0.497	0.205	−0.286	−0.081	−0.537	1.394	0.286
Ta—C**	2.207	2.216	0.097	0.161	0.086	−0.131	−0.045	−0.468	1.530	0.131
N—C**	1.416	1.418	0.274	−0.572	0.236	−0.614	−0.379	−1.384	2.607	0.614
Ta—S	2.645	2.646	0.056	0.104	0.041	−0.056	−0.015	−0.265	1.362	0.056
Ta—S	2.592	2.593	0.062	0.114	0.047	−0.065	−0.018	−0.297	1.392	0.065
Ta—S	2.639	2.641	0.057	0.105	0.041	−0.057	−0.015	−0.268	1.366	0.057
Ta—S	2.581	2.583	0.064	0.115	0.048	−0.068	−0.020	−0.309	1.408	0.068
Ta—S	2.587	2.588	0.063	0.115	0.047	−0.066	−0.019	−0.299	1.394	0.066
Ta—S	2.628	2.629	0.056	0.126	0.044	−0.057	−0.013	−0.232	1.292	0.057

* ρ is electron density; $\nabla^2\rho$ is the Laplacian; V , G , H are potential, kinetic [28], and total energy densities; the ρ and $\nabla^2\rho$ values are given in relative units (e/a_0^3 and e/a_0^5 , respectively).

** Bonds in the azametallacyclop propane moiety.

was determined by quantum chemical DFT calculations.

FUNDING

This study was supported by the Russian Academy of Sciences (budget program V55.1.1).

CONFLICT OF INTEREST

The authors declare that they have no conflicts of interest.

REFERENCES

1. Lappert, M., Protchenko, A., Power, P., and Seeber, A., *Metal Amide Chemistry*, Wiley, 2008.
2. Winter, C.H., *Aldrichimica Acta*, 2000, vol. 33, p. 3.
3. Nugent, W.A., Ovenall, D.W., and Holmes, S.J., *Organometallics*, 1983, vol. 2, p. 162.
4. Eisenberger, P., Ayinla, R.O., Lauzon, J.M.P., and Schafer, L.L., *Angew. Chem., Int. Ed.*, 2009, vol. 48, p. 8361.
5. Ahmed, K.J., Chisholm, M.H., Folting, K., and Huffman, J.C., *J. Chem. Soc., Chem. Commun.*, 1985, p. 152.
6. Cai, H., Chen, T., Wang, X., et al., *Chem. Commun.*, 2002, p. 230.
7. Wang, H., Wang, Y., Chan, H.-S., and Xie, Z., *Inorg. Chem.*, 2006, vol. 45, p. 5675.
8. Zhang, F., Song, H., and Zi, G., *Dalton Trans.*, 2011, vol. 40, p. 1547.
9. Gordon, A. and Ford, R., *The Chemist's Companion: A Handbook of Practical Data, Techniques, and References*, New York: Wiley, 1972.
10. Fulmer, G.R., Miller, A.J.M., Sherden, N.H., et al., *Organometallics*, 2010, vol. 29, p. 2176.
11. Petrov, P.A., Rogachev, A.V., Kompankov, N.B., et al., *Russ. J. Coord. Chem.*, 2017, vol. 43, p. 652. <https://doi.org/10.1134/S1070328417100074>
12. *APEX2 (version 1.08), SAINT (version 7.03), SADABS (version 2.11), SHELXTL (version 6.12)*, Madison: Bruker AXS Inc., 2004.
13. Sheldrick, G.M., *Acta Crystallogr., Sect. A: Found. Adv.*, 2015, vol. 71, p. 3.
14. Sheldrick, G.M., *Acta Crystallogr., Sect. C: Struct. Chem.*, 2015, vol. 71, p. 3.
15. Dolomanov, O.V., Bourhis, L.J., Gildea, R.J., et al., *J. Appl. Crystallogr.*, 2009, vol. 42, p. 339.
16. Velde, G.T., Bickelhaupt, F.M., Baerends, E.J., et al., *J. Comput. Chem.*, 2001, vol. 22, p. 931.

17. *ADF 2017. SCM. Theoretical Chemistry*, Amsterdam: Vrije Universiteit. <http://www.scm.com>.
18. Vosko, S.H., Wilk, L., and Nusair, M., *Can. J. Phys.*, 1980, vol. 58, p. 1200.
19. Becke, A.D., *Phys. Rev. A*, 1988, vol. 38, p. 3098.
20. Perdew, J.P., *Phys. Rev. B*, 1986, vol. 33, p. 8822.
21. Perdew, J.P., *Phys. Rev. B*, 1986, vol. 34, p. 7406.
22. Lenthe, E.V., Ehlers, A.E., and Baerends, E.J., *J. Chem. Phys.*, 1999, vol. 110, p. 8943.
23. Bradley, D.C. and Gitlitz, M.H., *Chem. Commun.*, 1965, p. 289.
24. Bradley, D.C. and Gitlitz, M.H., *J. Chem. Soc. A*, 1969, p. 1152.
25. Most, K., Mösch-Zanetti, N.C., Vidovic, D., and Maggall, J., *Organometallics*, 2003, vol. 22, p. 5485.
26. Bader, R.F.W., *Atoms in Molecules. A Quantum Theory*, Oxford: Clarendon, 1990.
27. Popelier, P., *Atoms in Molecules. An Introduction*, Harlow: Prentice Hall, 2000.
28. Abramov, Yu.A., *Acta Crystallogr., Sect. A: Found. Crystallogr.*, 1997, vol. 53, p. 264.

Translated by Z. Svitanko